



Visual perception of actions and objects has been shown to activate different cortical systems. Object recognition primarily relies on the ventral occipitotemporal cortex (VOTC)^{1,2}; Action observation activates predominantly the occipitoparietal region, posterior dorsal temporal gyrus and the inferior frontal gyrus (IFG)^{3,4}. VOTC has a well-established object “domain” organization, with different patches sensitive to several major, broad, evolutionarily-salient domains of objects (e.g., faces, animals, scenes and navigation-related large objects, small manipulable objects, with a broad animate/inanimate domain distinction)^{5–7}. Although the interaction between the visual ventral and dorsal pathways (what vs. how/where)^{8,9}, which overlapped with part of the action perception network, has been well documented^{10–18}, the evidence about whether action perception and its communication with the ventral object regions is also guided by parallel processing-domain-structure (social purpose vs. object purpose) is less clear-cut.

Several lines of evidence have suggested a domain-related interaction pattern between object and action perception systems. Different domains of objects activate dorsal regions that are implicated in action perception: Manipulable objects activated the inferior parietal lobe (IPL)⁴⁹ supporting manipulation knowledge of tools and hand-object action perception^{3,4,20–22}; faces and animals activated the posterior superior temporal sulcus (pSTS)²³ related to biological motion and social interaction perception^{4,22,24,25}. The structural or resting-state functional brain connectivity of ventral-object and dorsal-action systems were also organized into a domain-like pattern:

¹B. Zhang, Z. Li, J. Zhang, Y. Chen, D. Wang, X. Ma, H. Zhang, S. Li, C. Wang, B. Zhang, Beijing Normal University, Beijing 100875, China. ²B. Zhang, Z. Li, J. Zhang, Y. Chen, D. Wang, X. Ma, H. Zhang, S. Li, C. Wang, B. Zhang, Beijing Normal University, Beijing 100875, China.

tool-preferring ventral areas were connected with the frontoparietal hand-arm/manipulation action processing regions^{13,26–29}, and face-preferring ventral areas with the pSTS social cognition region³⁰. Functional connectivity (FC) between tool-preferring ventral and dorsal regions was enhanced during action-performing tasks^{12,14}. Recent studies have further shown the causal influence of the left inferior parietal areas on the ventral regions or object representations: lesions or stimulation to this region modulate the tool representations in the ventral-medial tool-preferring areas^{31,32}.

findings are only indirect evidence for whether action perception system itself is organized by “domains” and how it communicates with the ventral object system dynamically. Given that the studies reviewed above tended to involve object stimuli (e.g., object names, movies of real multi-object contexts, but see Centelles et al.²⁴), it is possible that these effects were driven by object-domain properties (e.g., animate/biological vs. artifact object). Objects are recognized by the ventral visual system, which is organized by the salient object domains (i.e., animate/inanimate), and activate the typical action knowledge about that object stored in the dorsal system through brain connections, or activate the parietal regions directly through subcortical pathways^{33,34}. It is thus not clear whether domains of actions are only organized along the animate/inanimate dimensions (a car moving vs. a person walking), or by domains that are beyond object properties, such as social-communicative-actions versus manipulation-actions³⁵. For instance, pSTS has been robustly implicated in biological motion^{36–39}, but it is unknown whether this region has different degree of sensitivities to different kinds of biological motion (social- vs. manipulation-actions). Note that Centelles et al.²⁴ have tried to exclude the effects of object properties and found stronger pSTS activations when participants watching two individuals interacting compared with two individuals acting independently using point-light stimuli. This comparison was between human-social-goal-directed versus non-goal-directed movements, whether pSTS differentiate different goal-directed biological motions (human-directed social-communicative-actions vs. object-directed manipulation-actions) is unknown. Also unclear is whether action perception entails dynamic functional communications between the dorsal action perception network with the ventral object processing stream in a domain-specific manner. Here, we test the hypothesis of a domain-organized action perception pathway using action stimuli excluding object domain differences, with an experiment designed to optimally evaluate both regional activities and task-based FC patterns. Participants watched videos of a human cartoon figure performing two types of actions (social-communicative-actions such as waving, manipulation-actions such as folding) to a same set of meaningless shapes during fMRI scanning. We examined whether the two action-perception conditions elicited different dorsal action perception system activations and whether such activations communicated with the ventral system differently.

First, both types of action perception conditions, compared to baseline, activated the bilateral IFG, superior parietal gyri, and posterior superior to inferior temporal gyri (voxel level $p < 0.0001$, cluster-extent FWE $p < 0.05$; Supplementary Fig. S1). We then carried out whole-brain univariate contrasts between conditions where participants watched videos of social-communicative-actions and manipulation-actions (voxel level $p < 0.0001$, cluster-extent FWE $p < 0.05$).

Social-communicative-actions video-watching. Social-communicative-actions, simulating human-human interaction such as waving, induced greater activation than manipulation-actions in the right precentral gyri (Prec), bilateral pSTS/posterior middle temporal gyrus (pMTG; Fig. 1a,c and Table 1).

Manipulation-actions video-watching. Manipulation-actions (e.g., folding an object) induced greater activation than social-communicative-actions in the bilateral supramarginal gyri (SMG), bilateral IPL, bilateral superior parietal lobe (SPL), bilateral postcentral gyri (Poc), bilateral Prec, right superior and inferior frontal gyri, and left insula (Fig. 1b,d and Table 1).

These results indicate that social-communicative-actions and manipulation-actions, without object-domain information (same set of human cartoon figure and arbitrary meaningless shapes), elicited different distributed activations across frontal, parietal and dorsal temporal regions. Worth-noting is that both the social-communicative-actions and the manipulation-actions activated bilateral pSTS relative to baseline (Supplementary Fig. S1), in line with previous findings that highlighted the role of pSTS in biological motions³⁶⁻³⁹. Importantly here, the pSTS showed stronger sensitivity to social-communicative-action perception, indicating effects beyond biological motion per se. Also note that even though the cartoon figure and meaningless shapes may have some form changes during the actions (e.g., Fig. 2a, the form of the shape changes when the cartoon figure acts on it in the manipulation-action condition), these form changes do not correspond to the object domain differences. They did, however, result in more cumulative movement information in this condition than the social-communicative-actions (see “Experimental design” section). To examine if any results for the manipulation action were simply due to sensitivity to more visual changes (movements), we looked at the navigation condition that were not of interest in the current study, which had even higher cumulative movements than the manipulation-actions ($p = 1.185 \times 10^{-29}$). We compared the activation strengths in those manipulation specific-activation regions between navigation condition and the manipulation-actions, with the rationale that if these regions simply responded to more actions, they should show higher responses to navigation than to manipulation actions. All but one of the manipulation specific-activation clusters showed higher activations for the manipulation-actions or no differences with the navigation, indicating that the manipulation-action-specific effects in these regions were not simply attributable to more movements in video stimuli (Supplementary Fig. S5a). The one exception located in the right IFG/Prec (MNI peak coordinates: 54, 9, 24), showing stronger activation in the navigation

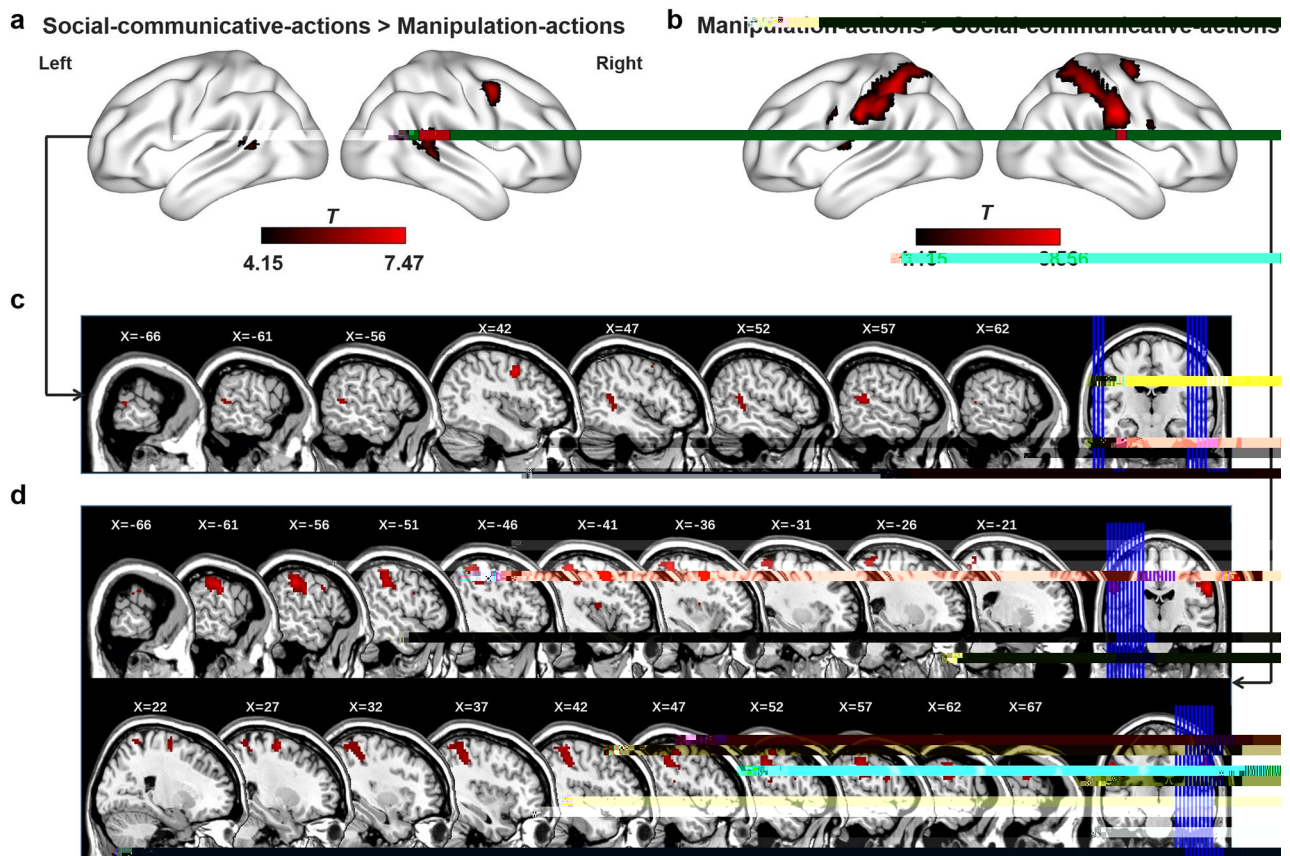
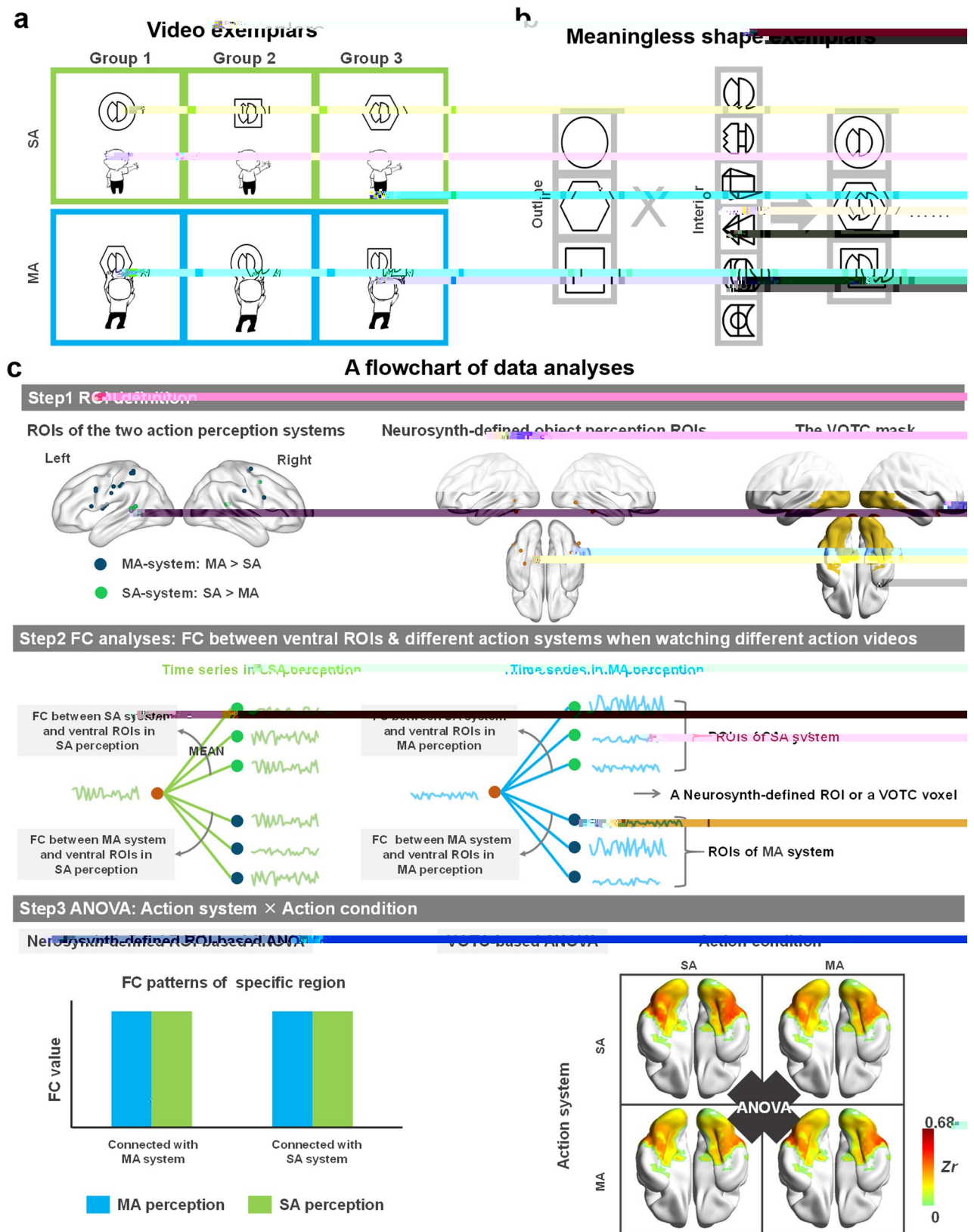


Figure 1. Whole brain univariate analysis results of social- and manipulation-action perception. **a,c** Cortical surface and multi-slice presentation of social-communicative-action specific activation relative to the manipulation-action condition. **b,d** Cortical surface and multi-slice presentation manipulation-action specific activation relative to the social-communicative-action condition. Threshold: voxel level $p < 0.0001$, cluster-extent FWE corrected $p < 0.05$.

Contrast	Anatomical regions of the cluster's peak voxel (other including regions)	MNI coordinates of peak voxel (mm)			t	Cluster size
		x	y	z		
SA versus MA	Right Prec	42	3	45	7.47	43
	Right STG (MTG)	57	-42	15	5.73	71
	Le MTG	-66	-42	9	5.09	20
MA versus SA	Right Posc (IPL; SMG; SPL)	60	-18	33	8.56	459
	Le SPL (Posc; IPL, SMG)	-36	-45	60	8.17	462
	Right SFG (Prec)	27	-9	63	6.80	52
	Le Prec	-54	6	36	5.76	15
	Right IFoper (Prec)	54	9	24	5.46	21
	Le insular (rolandic oper)	-39	-6	12	5.10	16

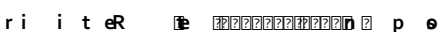
Table 1. Whole-brain univariate analysis results of social- or manipulation-action-specific activations. threshold: voxel level $p < 0.0001$, cluster-extent FWE corrected $p < 0.05$. SA social-communicative-actions, MA manipulation-actions, Prec precentral gyrus, STG superior temporal gyrus, MTG middle temporal gyrus, Posc postcentral gyrus, IPL inferior parietal lobe, SMG supramarginal gyrus, SPL superior parietal lobe, SFG superior frontal gyrus, IFoper inferior frontal operculum.

than in the manipulation-actions. We thus performed additional validation analyses excluding this cluster in the FC analyses (ROI-based) below, and the results were fully replicated (Supplementary Fig. S5b–e).





communicates with the ventral object perception regions in a domain-specific manner, we calculated the FC strength between the two action systems obtained for each participant (see “Methods” section) and VOTC in different task conditions. That is, for each Neurosynth-defined object domain ROI (in the ROI analysis) or each VOTC voxel (in the whole VOTC mask analysis) we obtained four FC measures: FC strength with the two action systems (social-communicative-action and manipulation-action) in the two video conditions (social-communicative-action perception; manipulation-action perception) and applied a 2×2 repeated-measure ANOVA (Fig. 2c). Only those results showing statistical significance are reported below.


ROI analysis results. To examine whether action perception system connected with ventral object perception regions in a domain-specific manner from a theory-driven perspective, analyses were carried out on VOTC ROIs showing face- or tool-preferring activations, defined by Neurosynth meta-analyses (Fig. 3, Supplementary Table S4; see also Methods). Face preferring ROI (bilateral FFA) and tool preferring ROI (left LOTC) showed significant interaction effects between action perception system and action viewing conditions (left FFA, $F(35) = 7.699$,




ri i t eR  <https://doi.org/10.1038/s41598-020-78276-4>

ri i t eR  <https://doi.org/10.1038/s41598-020-78276-4> nature research 6

ri i t eR  <https://doi.org/10.1038/s41598-020-78276-4> nature research 6

ri i t eR  <https://doi.org/10.1038/s41598-020-78276-4> nature research 6

ri i t eR  <https://doi.org/10.1038/s41598-020-78276-4> nature research 6

ri i t eR te ??????????n ? p e

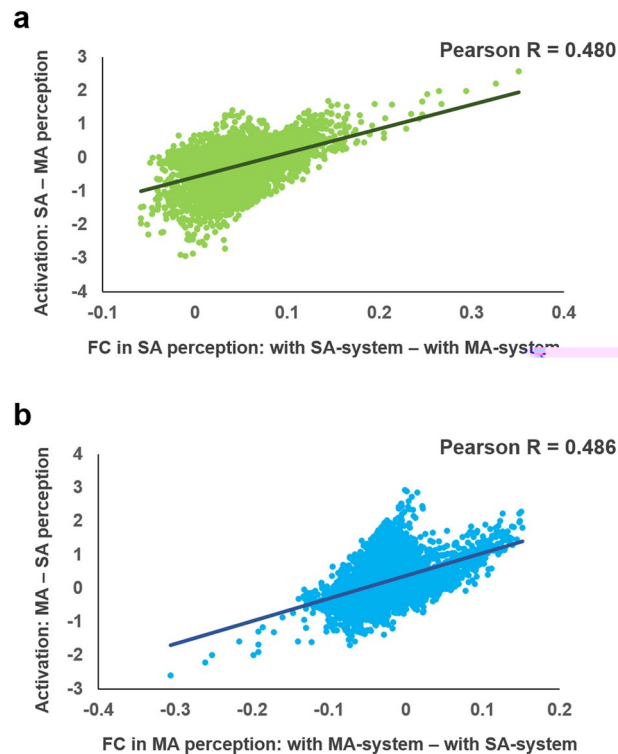


Figure 5. Correlation between the domain-specific FC (connected with one of the action systems relative to the other one in the corresponding action perception condition) and domain-specific local activation strength (in one action condition relative to the other) across VOTC voxels. Correlations for both domains (social vs. manipulation) were significant ($p < 5.550 \times 10^{-225}$). Each dot represents a VOTC voxel ($N = 3915$), with green dots for the social-communicative-action domain and blue dots for the manipulation-action domain. SA social-communicative-action perception, MA manipulation-action perception.

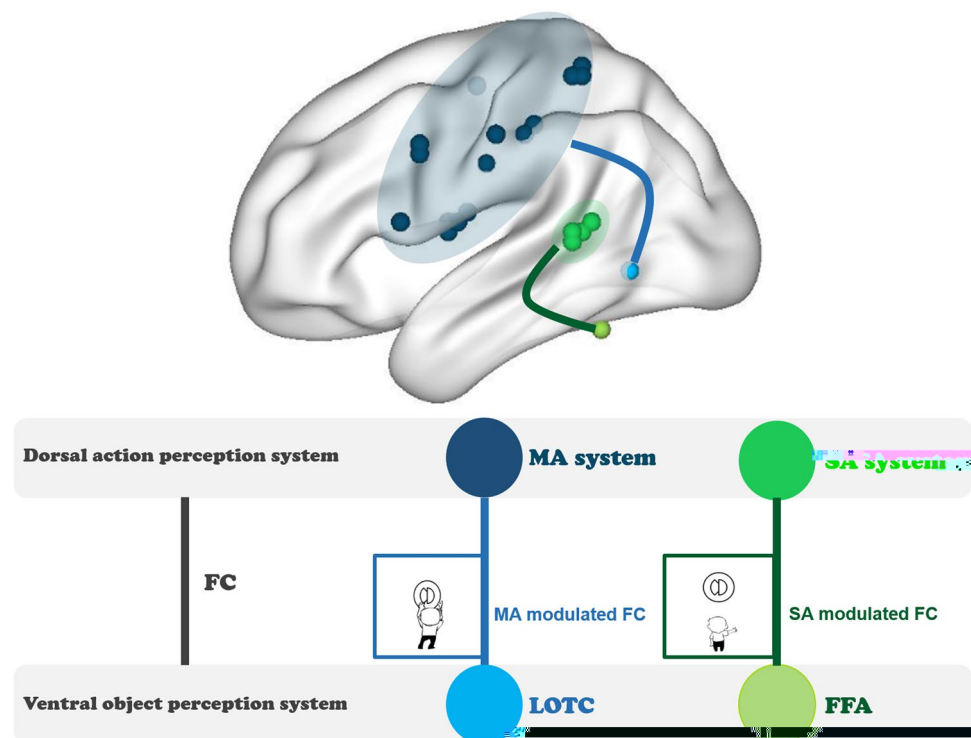


Figure 6. Summary of the FC patterns between the dorsal action perception system and the ventral object perception regions. MA manipulation-actions, SA social-communicative-actions.

uted to properties of the corresponding object domains (i.e., animate/biological vs. artifact shape properties), but related to the different types of action patterns or action consequences. Our manipulation-actions, in order to be natural, caused the target to go through a form change as a mechanical consequence of manipulation.

in the post-experimental survey of our study. Most of them named the meaningless shapes according to their shapes (e.g. diamond) and then establish relationship between the actions and shapes through rote learning.

li e current results of social- versus manipulation-action domain organization in the action perceptual system (parietal, frontal, and dorsal temporal cortex), domain-specific functional-connection pattern with the ventral object pathway, together with the classical object domain-organization in the ventral visual pathway (faces in FFA vs. manipulable small objects in LOTC), reflect a unified principle in perception: social-versus manipulation- domains. This is in accord with the general notion of the connectivity-constrained domain representation hypothesis⁴⁷. Previously, “domain” has been used usually in the context of object representation (conspicuous, tools, animals, etc.). Our findings highlight the significance of domains of human-interaction as an overarching principle: Object-manipulation and social-interaction for both ventral and dorsal visual perception system, and demonstrate domain-based dynamic functional communication across systems⁴⁸.

Participants Forty-four right-handed individuals (20 males; 22.4 ± 2.4 years old, range 18–28 years old) with normal or corrected-to-normal vision participated in this study. Forty-six (15 males; 22.2 ± 2.4 years old, range 18–28 years old) of them were included in the following analyses. Eight participants were excluded for excessive head-motion and balance of the action-shape matching rules (see the following parts and Supplementary Table S1 for details). Results of using more liberal participant inclusion criteria using forty-two participants (i.e. excluding only the two participants with excessive head-motion) were largely similar (Supplementary Fig. S2). None reported psychiatric or neurological disorders. All participants gave written informed consent and were paid for their participation. The protocol was approved by the Institutional Review Board of the Beijing MRI Center for Brain Research. All methods were performed in accordance with relevant named guidelines and regulations.

Experiment 1 Participants viewed two kinds of action videos (social interaction and object-manipulation), with both the agent and object held constant (a human figure and an arbitrary meaningless shape). Videos were made by a professional animation company and included actions performed by the same cartoon figure towards the meaningless shapes (see Fig. 2a for screenshot; all video stimuli were shown in Supplementary Fig. S1). The actions correspond to two domains, with six actions in each type: social-communicative-actions (waving; saluting; bowing; kissing; clapping; greeting) and manipulation-actions (folding; tearing; overturning; rotating; pressing upper and lower; pressing left and right). The experiment also included a third navigation condition for other interests and were not considered for the main analyses. Each meaningless shape consisted of an outline and an interior shape (see exemplars in Fig. 2b). Six different interior meaningless shapes⁴⁹ were combined with three different outline shapes (hexagon, circle, and square) to form the meaningless shapes. To verify the sociality of the social-communicative-actions, we collected sociality ratings on a 7-point scale (how likely these actions are directed at people, 1 = never, 7 = always) in an independent group of participants ($N = 23$, 16 females, mean age = 22.9). The social-communicative-action condition was indeed rated to be significantly more person-directed than the manipulation-action condition [mean ratings 6.04 ± 0.65 vs. 3.02 ± 1.55 ; $t(22) = 9.104$, $p = 6.468 \times 10^{-9}$]. The participants were instructed to remember the correspondence between action and shape. They were asked to report the action name associated with the presented shape and simulate the action after scanning. The three types of meaningless shapes (outlines) were counterbalanced across action types in a between-participant fashion (Fig. 2a), such that meaningless shapes included in the different action types were fully matched at the group level. Equal number of participants in each action-shape matching group. It should be noted that in the manipulation-action condition, the action induced shape to change form, as an intrinsic consequence of manipulation. These visual shape changes made the cumulative movements significantly higher in the manipulation-action than the social-communicative-action condition (sum of the amount of changes of the whole stimuli for each frame relative to the previous one; absolute value of pixel changes: $p = 1.644 \times 10^{-7}$). While this difference (i.e., form changes of meaningless shape in the manipulation-actions but not in the social-communicative-actions) did not correspond to any known domain differences between inanimate and animate objects, we further considered the potential effects of this confounding variable (amount of visual changes) on action domain effects by looking at another condition of no-interest where the amount of visual changes were even greater than the manipulation action condition (see “Results” section).

A long-block experimental design was employed, with 36 time points for each block. This allowed enough number of time points to calculate time series correlation without needing to concatenate different blocks from the same condition. This design is optimal to evaluate both regional activities and task-based FC^{50–52}. The video-watching task included 4 runs. Each run consisted of a 10 s fixation dot presented centrally, followed by 3 blocks from the different action conditions. Each block consisted of 24 trials from the same condition (i.e., each exemplar was repeated 4 times), followed by 10 s fixation. Each 3000-ms trial consisted of an action stimulus that lasted for 2000 ms, followed by 1000 ms of standing still (or running without turning in the navigation condition). The trial order was random and the block order was counterbalanced in a Latin square fashion across runs and participants. The experimental procedure was presented using Psychtoolbox (<http://psychtoolbox.org/>) implemented in MATLAB (<https://www.mathworks.com/products/matlab.html>).

Procedure The whole scanning session for each participant was about 95 min: (a) resting functional MRI scan; (b) meaningless shape viewing scan; (c) T1 functional scan; (d) video-watching scan (main experiment); (e) meaningless shape viewing scan; (f) diffusion tensor imaging. Data of procedure a, b, e, f were designed for another question and not analyzed herein. Whole scan data were acquired

Functional images were preprocessed using Statistical Parametric Mapping (SPM12, <http://www.lion.ucl.ac.uk/spm>). The first 5 volumes in each run were discarded. Three-dimensional head-motion correction was conducted with respect to the mean volume of each run. Two participants were excluded for excessive head motion (above 2 mm or 2°). No other participants exhibited excessive head motion (<1.47 mm or 1.11°). For each participant, T1 images were co-registered to their mean functional images and were subsequently segmented. Functional images were normalized to the Montreal Neurological Institute (MNI) space using T1 image unified segmentation. After normalization, functional images were resampled to $3 \times 3 \times 3 \text{ mm}^3$ and spatially smoothed with a 6 mm Full Width Half Maximum Gaussian filter. For FC analyses, the following preprocessing steps were additionally performed: linear trend removal, band-pass filtering (0.01–0.1 Hz), and regression of eight nuisance covariates (six rigid-body head-motion parameters, white matter signal, and cerebrospinal fluid signal). Global signal regression is controversial^{53,54} and often causes ‘negative’ correlations among brain regions. Therefore, we did connectivity analyses using data without global signal removal and repeated the analyses with global signal regression as validation analyses (see validation results in Supplementary Figs. S6 and S7; Supplementary Table S2). The residual time series with these nuisance covariates regression were used to do FC analyses.

To explore how the domain-specific action perception systems communicate with the ventral object perception regions during action perception, we carried out task-state FC analyses. Specifically, we calculated the FC, seeding from the social- or manipulation-action perception systems, with ventral object perception regions during the two video conditions. We then applied repeated-measure ANOVAs to these FC measures. Figure 2c shows a flowchart of these analyses.

We considered ventral object perception regions in two ways: (1) In a ROI approach, we defined classical regions showing preference for social entities and manipulable objects/tools using the Neurosynth meta-analyses platform (<https://neurosynth.org>). Specifically, we searched for the terms “face” and “tool” separately in Neurosynth and retrieved the association threshold maps (896 studies including the word “face” and “115” studies including the word “tools”; default threshold at FDR corrected, $p < 0.01$). It should be noted that we also used “artifacts” or “manipulable objects” to search, but no results were found. We used “tools” rather than “objects” because the former is more specific to manipulation actions. These maps were resliced into the same voxel size with the functional images, i.e., $3 \times 3 \times 3 \text{ mm}^3$. The strongest peaks within VOTC for “face” were in the bilateral lateral fusiform gyrus (i.e., fusiform face area, FFA), and for “tools” in the left lateral occipitotemporal cortex (LOTc; Supplementary Fig. S4; Table S4). These peaks were extracted and used to form sphere ROIs of 3 mm radius. A small significant cluster for tool in the medial fusiform gyrus (medFG) was further included given its relevance highlighted in previous literature^{12,29,56}; (2) in a data-driven approach, we used a whole VOTC mask,

obtained using previous dataset in our lab, to test the dynamic FC patterns of dorsal action perception system and ventral object perception system. It was defined by combining functional and anatomical localization, including regions that were activated during an object picture perception task within the occipitotemporal cortex (z coordinate below 10; see Wang et al.⁵⁷, procedure following Kriegeskorte et al.⁵⁸).

FC computation. The following steps were carried out in each participant separately. First, the task-state residual time series of each run was segmented into separate conditions as follows: for each block in each run, the first 4 volumes (8 s) were discarded, and 2 volumes (4 s) of the 10 s fixation were included to account for the hemodynamic delay. Within each ROI sphere of the action systems, the residual time series of all voxels were averaged. Then, we computed the FCs seeding from each social- or manipulation-action perception ROI sphere with each Neurosynth-defined ventral object domain ROI (in the ROI analysis), or each voxel in the VOTC mask (in the Whole VOTC mask analysis), under the two action perception conditions separately. The correlation coefficients were then Fisher-z transformed and averaged across all ROIs within an action system, across all runs within an experiment condition, to yield four measures for each ventral ROI or voxel (Fig. 2c): FC with the social-communicative-action system in the social-communicative-action condition, FC with the social-communicative-action system in the manipulation action condition, FC with the manipulation-action system in the social-communicative-action condition, FC with the manipulation-action system in the manipulation-action condition. Note that in the main analysis, multiple ROIs in the same action systems were averaged together for the ANOVA analysis. We also report the FC results between each separate action perception ROI sphere and each Neurosynth-defined object perception ROI (Supplementary Fig. S9).

ANOVA. For Neurosynth-defined ventral classical object perception ROIs, we applied repeated-measure ANOVAs using SPSS Statistics 20 (<https://www.ibm.com/cn-zh/analytics/spss-statistics-software>) to test whether social- and manipulation-action perception systems interact with face and tool perception regions in a domain-specific way. We then applied repeated-measure ANOVAs using SPM12 to identify brain regions showing significant main effects of action brain system/action perception condition or interaction effects between the action brain system and action perception condition within whole VOTC mask (threshold set as voxel level $p < 0.001$, cluster-extent FWE corrected $p < 0.05$). For regions showing significant interaction effects, subsequent comparisons were performed (two-tailed paired-sample *t*-tests) to test the specific connection patterns among the four FC conditions (all Bonferroni-corrected based on four comparisons of simple effects).

Results

FC strength and VOTC activation. To examine whether dorsal action systems could affect the VOTC activation through functional coupling when object-domain information had been well-controlled, we calculated the correlation between FC strength with a specific action system and activation strength in each action perception conditions across VOTC voxels. First, for each VOTC voxel we calculated its average FC strength across all participants for each of the four measures (with two action systems in two conditions). Then, for each VOTC voxel we calculated the average activation strength across participants for social-communicative-action and manipulation-action perception conditions separately. Then we computed the Pearson correlation coefficient between the domain-specific FC strength (i.e., connected with one of the action systems relative to the other one in the same action perception condition) and the domain-specific activation strength (i.e., in one action condition relative to the other) across all of the VOTC voxels.

Availability of data and materials

The data that support the results of the present study are available from the corresponding author upon reasonable request.

Received: 14 August 2020; Accepted: 9 November 2020
Published online: 03 December 2020

References

- Downing, P. E., Chan, A.-Y., Peelen, M., Dodds, C. & Kanwisher, N. Domain specificity in visual cortex. *Cereb. Cortex* **16**, 1453–1461. <https://doi.org/10.1093/cercor/bhj086> (2005).
- Spiridon, M., Fischl, B. & Kanwisher, N. Location and spatial profile of category-specific regions in human extrastriate cortex. *Hum. Brain Mapp.* **27**, 77–89. <https://doi.org/10.1002/hbm.20169> (2006).
- Caspers, S., Zilles, K., Laird, A. R. & Eickhoop, S. B. ALE meta-analysis of action observation and imitation in the human brain. *Neuroimage* **50**, 1148–1167. <https://doi.org/10.1016/j.neuroimage.2009.12.112> (2010).
- Grosbras, M. H., Beaton, S. & Eickhoop, S. B. Brain regions involved in human movement perception: a quantitative voxel-based meta-analysis. *Hum. Brain Mapp.* **33**, 431–454. <https://doi.org/10.1002/hbm.21222> (2012).
- Epstein, R. & Kanwisher, N. A cortical representation of the local visual environment. *Nature* **392**, 598–601. <https://doi.org/10.1038/33402> (1998).
- Kanwisher, N., McDermott, J. & Chun, M. M. The fusiform face area: a module in human extrastriate cortex specialized for face perception. *J. Neurosci.* **17**, 4302–4311. <https://doi.org/10.1523/JNEUROSCI.17-11-04302.1997> (1997).
- Konkle, T. & Caramazza, A. Tripartite organization of the ventral stream by animacy and object size. *J. Neurosci.* **33**, 10235–10242. <https://doi.org/10.1523/JNEUROSCI.0983-13.2013> (2013).
- Goodale, M. A. & Milner, A. D. Separate visual pathways for perception and action. *Trends Neurosci.* **15**, 20–25. [https://doi.org/10.1016/0166-2236\(92\)90344-8](https://doi.org/10.1016/0166-2236(92)90344-8) (1992).
- Ungerleider, L. G. & Mishkin, M. Two cortical visual systems. Analysis of visual behavior. Ingle DJ, Goodale MA, Mansfield RJW (1982).
- Chen, Q., Garcea, F. E., Almeida, J. & Mahon, B. Z. Connectivity-based constraints on category-specificity in the ventral object processing pathway. *Neuropsychologia* **105**, 184–196. <https://doi.org/10.1016/j.neuropsychologia.2016.11.014> (2017).

11. Freud, E., Plaut, D. C. & Behrmann, M. 'What's happening in the dorsal visual pathway. *Trends Cogn. Sci.* **20**, 773–784. <https://doi.org/10.1016/j.tics.2016.08.003> (2016).
12. Garcea, F. E., Chen, Q., Vargas, R., Narayan, D. A. & Mahon, B. Z. Task- and domain-specific modulation of functional connectivity in the ventral and dorsal object-processing pathways. *Brain Struct. Funct.* **223**, 2589–2607. <https://doi.org/10.1007/s00429-018-1641-1> (2018).
13. Hutchison, R. M., Culham, J. C., Everling, S., Flanagan, J. R. & Gallivan, J. P. Distinct and distributed functional connectivity patterns across cortex reflect the domain-specific constraints of object, face, scene, body, and tool category-selective modules in the ventral visual pathway. *Neuroimage* **96**, 216–236. <https://doi.org/10.1016/j.neuroimage.2014.03.068> (2014).
14. Hutchison, R. M. & Gallivan, J. P. Functional coupling between frontoparietal and occipitotemporal pathways during action and perception. *Cortex* **98**, 8–27. <https://doi.org/10.1016/j.cortex.2016.10.020> (2018).
15. Lingnau, A. & Downing, P. E. The lateral occipitotemporal cortex in action. *Trends Cogn. Sci.* **19**, 268–277. <https://doi.org/10.1016/j.tics.2015.03.006> (2015).
16. Mahon, B. Z., Kumar, N. & Almeida, J. Spatial frequency tuning reveals interactions between the dorsal and ventral visual systems. *J. Cogn. Neurosci.* **25**, 862–871. https://doi.org/10.1162/jocn_a.00370 (2013).
17. Saygin, Z. M. *et al.* Anatomical connectivity patterns predict face selectivity in the fusiform gyrus. *Nat. Neurosci.* **15**, 321. <https://doi.org/10.1038/nn.3001> (2012).
18. Kravitz, D. J., Saleem, K. S., Baker, C. I. & Mishkin, M. A new neural framework for visuospatial processing. *Nat. Rev. Neurosci.* **12**, 217–230. <https://doi.org/10.1167/11.11.923> (2011).
19. Chao, L. L. & Martin, A. Representation of manipulable man-made objects in the dorsal stream. *Neuroimage* **12**, 478–484. <https://doi.org/10.1006/nimg.2000.0635> (2000).
20. Lewis, J. W. Cortical networks related to human use of tools. *Neuroscientist* **12**, 211–231. <https://doi.org/10.1177/1073858406288327> (2006).
21. Wang, X., Zhuang, T., Shen, J. & Bi, Y. Disentangling representations of shape and action components in the tool network. *Neuropsychologia* **117**, 199–210. <https://doi.org/10.1016/j.neuropsychologia.2018.05.026> (2018).
22. Wurm, M. F., Caramazza, A. & Lingnau, A. Action categories in lateral occipitotemporal cortex are organized along sociality and transitivity. *J. Neurosci.* **37**, 562–575. <https://doi.org/10.1523/JNEUROSCI.1717-16.2016> (2017).
23. Haxby, J. V., Ho-man, E. A. & Gobbini, M. I. The distributed human neural system for face perception. *Trends Cogn. Sci.* **4**, 223–233. [https://doi.org/10.1016/S1364-6613\(00\)01482-0](https://doi.org/10.1016/S1364-6613(00)01482-0) (2000).
24. Centelles, L., Assaiante, C., Nazarian, B., Anton, J. L. & Schmitz, C. Recruitment of both the mirror and the mentalizing networks when observing social interactions depicted by point-lights: a neuroimaging study. *PLoS ONE* **6**, 10. <https://doi.org/10.1371/journal.pone.0015749> (2011).
25. Iacoboni, M. *et al.* Watching social interactions produces dorsomedial prefrontal and medial parietal BOLD fMRI signal increases compared to a resting baseline. *Neuroimage* **21**, 1167–1173. <https://doi.org/10.1016/j.neuroimage.2003.11.013> (2004).
26. Bi, Y. *et al.* The white matter structural network underlying human tool use and tool understanding. *J. Neurosci.* **35**, 6822–6835. <https://doi.org/10.1523/JNEUROSCI.3709-14.2015> (2015).
27. Peelen, M. V. *et al.* Tool selectivity in the lateral occipitotemporal cortex develops without vision. *J. Cogn. Neurosci.* **25**, 1225–1234. https://doi.org/10.1162/jocn_a.00411 (2013).
28. Simmons, W. K. & Martin, A. Spontaneous resting-state BOLD fluctuations reveal persistent domain-specific neural networks. *Soc. Cognit. Affect. Neurosci.* **7**, 467–475. <https://doi.org/10.1093/scan/nsr018> (2012).
29. Stevens, W. D., Tessler, M. H., Peng, C. S. & Martin, A. Functional connectivity constrains the category-related organization of human ventral occipitotemporal cortex. *Hum. Brain Mapp.* **36**, 2187–2206. <https://doi.org/10.1002/hbm.22764> (2015).
30. Turk-Browne, N. B., Norman-Haignere, S. V. & McCarthy, G. Face-specific resting functional connectivity between the fusiform gyrus and posterior superior temporal sulcus. *Front. Hum. Neurosci.* **4**, 176. <https://doi.org/10.3389/fnhum.2010.00176> (2010).
31. Garcea, F. E. *et al.* Domain-specific diaschisis: Lesions to parietal action areas modulate neural responses to tools in the ventral stream. *Cereb. Cortex* **29**, 3168–3181. <https://doi.org/10.1093/cercor/bhy183> (2019).
32. Lee, D., Mahon, B. Z. & Almeida, J. Action at a distance on object-related ventral temporal representations. *Cortex* **117**, 157–167. <https://doi.org/10.1016/j.cortex.2019.02.018> (2019).
33. Almeida, J., Fintzi, A. R. & Mahon, B. Z. Tool manipulation knowledge is retrieved by way of the ventral visual object processing pathway. *Cortex* **49**, 2334–2344. <https://doi.org/10.1016/j.cortex.2013.05.004> (2013).
34. Fang, F. & He, S. Cortical responses to invisible objects in the human dorsal and ventral pathways. *Nat. Neurosci.* **8**, 1380–1385. <https://doi.org/10.1038/nn1537> (2005).
35. Wurm, M. F. & Caramazza, A. Distinct roles of temporal and frontoparietal cortex in representing actions across vision and language. *Nat. Commun.* **10**, 1–10. <https://doi.org/10.1016/361220> (2019).
36. Beauchamp, M. S., Lee, K. E., Haxby, J. V. & Martin, A. Parallel visual motion processing streams for manipulable objects and human movements. *Neuron* **34**, 149–159. [https://doi.org/10.1016/S0896-6273\(02\)00642-6](https://doi.org/10.1016/S0896-6273(02)00642-6) (2002).
37. Grossman, E. D., Battelli, L. & Pascual-Leone, A. Repetitive TMS over posterior STS disrupts perception of biological motion. *Vis. Res.* **45**, 2847–2853. <https://doi.org/10.1016/j.visres.2005.05.027> (2005).
38. Han, Z. *et al.* Distinct regions of right temporal cortex are associated with biological and human-agent motion: functional magnetic resonance imaging and neuropsychological evidence. *J. Neurosci.* **33**, 15442–15453. <https://doi.org/10.1523/JNEUROSCI.5868-12.2013> (2013).
39. Saygin, A. P. Superior temporal and premotor brain areas necessary for biological motion perception. *Brain* **130**, 2452–2461. <https://doi.org/10.1093/brain/awm162> (2007).
40. Isik, L., Koldewyn, K., Beeler, D. & Kanwisher, N. Perceiving social interactions in the posterior superior temporal sulcus. *Proc. Natl. Acad. Sci.* **114**, E9145–E9152. <https://doi.org/10.1073/pnas.1714471114> (2017).
41. Egorova, N., Shtyrov, Y. & Pulvermüller, F. Brain basis of

49. Song, Y., Bu, Y., Hu, S., Luo, Y. & Liu, J. Short-term language experience shapes the plasticity of the visual word form area. *Brain Res.* **1316**, 83–91. <https://doi.org/10.1016/j.brainres.2009.11.086> (2010).
50. Gonzalez-Castillo, J. *et al.* Tracking ongoing cognition in individuals using brief, whole-brain functional connectivity patterns. *Proc. Natl. Acad. Sci.* **112**, 8762–8767. <https://doi.org/10.1073/pnas.1501242112> (2015).
51. Liang, X., Zou, Q., He, Y. & Yang, Y. Coupling of functional connectivity and regional cerebral blood flow reveals a physiological basis for network hubs of the human brain. *Proc. Natl. Acad. Sci.* **110**, 1929–1934. <https://doi.org/10.1073/pnas.1214900110> (2013).
52. Wang, X. *et al.* Representing object categories by connections: evidence from a multivariate connectivity pattern classification approach. *Hum. Brain Mapp.* **37**, 3685–3697. <https://doi.org/10.1002/hbm.23268> (2016).
53. Fox, M. D., Zhang, D., Snyder, A. Z. & Raichle, M. E. The global signal and observed anticorrelated resting state brain networks. *J. Neurophysiol.* **101**, 3270–3283. <https://doi.org/10.1152/jn.90777.2008> (2009).
54. Murphy, K., Birn, R. M., Handwerker, D. A., Jones, T. B. & Bandettini, P. A. The impact of global signal regression on resting state correlations: are anti-correlated networks introduced? *Neuroimage* **44**, 893–905. <https://doi.org/10.1016/j.neuroimage.2008.09.036> (2009).
55. Xia, M., Wang, J. & He, Y. BrainNet Viewer: a network visualization tool for human brain connectomics. *PLoS ONE* **8**, e68910. <https://doi.org/10.1371/journal.pone.0068910> (2013).
56. Chao, L. L., Haxby, J. V. & Martin, A. Attribute-based neural substrates in temporal cortex for perceiving and knowing about objects. *Nat. Neurosci.* **2**, 913–919. <https://doi.org/10.1038/13217> (1999).
57. Wang, X. *et al.* How visual is the visual cortex? Comparing connective and functional fingerprints between congenitally blind and sighted individuals. *J. Neurosci.* **35**, 12545–12559. <https://doi.org/10.1523/JNEUROSCI.3914-14.2015> (2015).
58. Kriegeskorte, N. *et al.* Matching categorical object representations in inferior temporal cortex of man and monkey. *Neuron* **60**, 1126–1141. <https://doi.org/10.1016/j.neuron.2008.10.043> (2008).

manuscript

This study was funded by the National Natural Science Foundation of China (31671128 to Y.B.), Changjiang Scholar Professorship Award (T2016031 to Y.B.), the 111 Project (BP0719032 to Y.B.), China Postdoctoral Science Foundation (2020M670190 to H.Y.) and the Fundamental Research Funds for the Central Universities (2017STUD33 to H.Y.). We thank all Bi lab members, especially Xiaosha Wang and Xiaoying Wang for helpful comments on earlier versions of the manuscript.

contributions

Y.B. and Z.H. designed the experiment. H.Y. and C.H. did data acquisition and analysis. Y.B. and H.Y. drafted the paper and substantively revised it.

Competing interests

The authors declare no competing interests.

Additional information

Supplementary information is available for this paper at <https://doi.org/10.1038/s41598-020-78276-4>.

Correspondence and requests for materials should be addressed to Y.B.

Reprints and permissions information is available at www.nature.com/reprints.

Publisher's note Springer Nature remains neutral with regard to jurisdictional claims in published maps and institutional affiliations.



Open Access This article is licensed under a Creative Commons Attribution 4.0 International License, which permits use, sharing, adaptation, distribution and reproduction in any medium or format, as long as you give appropriate credit to the original author(s) and the source, provide a link to the Creative Commons licence, and indicate if changes were made. The images or other third party material in this article are included in the article's Creative Commons licence, unless indicated otherwise in a credit line to the material. If material is not included in the article's Creative Commons licence and your intended use is not permitted by statutory regulation or exceeds the permitted use, you will need to obtain permission directly from the copyright holder. To view a copy of this licence, visit <http://creativecommons.org/licenses/by/4.0/>.

© The Author(s) 2020